

SOLITON TUNNELING

G. KÄLBERMANN
Faculty of Agriculture
and

Racah Institute of Physics
Hebrew University, 91904 Jerusalem, Israel

February 26, 2018

Abstract

We present a numerical simulation of the scattering of a topological soliton off finite size attractive impurities, repulsive impurities and a combination of both. The attractive and attractive-repulsive cases show similar features to those found for δ function type of impurities. For the repulsive case, corresponding to a finite width barrier, the soliton behaves completely classically. No tunneling occurs for sub-barrier kinetic energies despite the extended nature of the soliton.

PACS 03.40.Kf, 73.40.Gk, 23.60.+e

Topological solitons are frequently mentioned as possible candidates for the description of particles. Very notably the skyrmion [1, 2] has been proposed as a sound model of the nucleon. The topology of the skyrmion serves as a classical picture of the baryon current. It is quite clear that if nucleons can be considered as solitons in a nonlinear chiral lagrangian, their behavior in nuclei has to follow from the same framework. In particular one of the most intriguing characteristics of the quantum mechanical behavior of nucleons in nuclei is the tunneling through a barrier. The quantum picture of the nucleon as a wave allows for clear predictions of the tunneling rates for sub-barrier energies. The question then arises as to what would be the behavior of solitons colliding with a barrier in similar circumstances. In particular a soliton model can provide some partial answers on the longstanding problems of the tunneling times around which there is much controversy in the literature [3]. If the soliton is to behave as a classical particle, then there can not be sub-barrier tunneling at all. However, for an extended object the answer is not so straightforward (recall a high jumper whose center of mass goes through the barrier, while the jumper glides above it). The simplest case of such a process would be a one dimensional collision of a topological soliton-like the kink or the sine-gordon soliton- with a barrier. Such processes can be catalogued under the title of soliton-impurity interactions.

Some time ago Kivshar et al.[4] investigated the scattering of a kink and a sine-Gordon soliton off an attractive δ function well and found extremely interesting results, such as the existence of resonant behavior of the soliton, trapping, reflection and excitation of the so-called impurity modes. The use of a δ function impurity allowed them to predict analytically the existence of windows of reflection in between trapping and resonances regions as a function of impinging velocity, defying a classical interpretation as particle behavior. They did not consider a finite well nor the barrier case. The results found for the sine-Gordon and the kink models were essentially the same. Extensions of the model to include inhomogeneities were undertaken

in ref.[5]. An investigation of the chaotic behavior of the residence time of the soliton inside an attractive impurity as a function of initial location was performed by Fukushima and Yamada [6].

In the present work we calculate numerically the interaction of a kink with a finite width impurity of the attractive, repulsive, or mixed case. The basic model is described by the lagrangian

$$\mathcal{L} = \frac{1}{2}\partial_\mu\phi\partial^\mu\phi + \frac{1}{4}\Lambda\left(\phi^2 - \frac{m^2}{\lambda}\right)^2 \quad (1)$$

Here

$$\Lambda = \lambda + U(x) \quad (2)$$

λ being a constant, and $U(x)$ the impurity potential,

$$U(x) = h_1 \cosh\left(\frac{x-x_1}{a_1}\right)^{-2} + h_2 \cosh\left(\frac{x-x_2}{a_2}\right)^{-2} \quad (3)$$

allowing a combination of both repulsive $h_1 > 0$ and attractive $h_2 < 0$ impurities.

The partial differential equations of motion were solved using a finite difference method checked against the results of Kivshar et al. [4] (although we do not agree entirely with the actual values of the final velocities quoted there) and the free analytical solution. We took a soliton initially at $x = -3$ shot to the right with initial velocity v onto an impurity located at $x = 3$. The spatial boundaries were taken to be $-40 < x < 40$, with a grid of $dx = 0.04$ and a time lapse of $dt = 0.02$ up to a maximal time of $T = 200$ (10000 time steps). This choice proved efficient in preventing numerical instabilities and still not exceedingly time consuming. The upper time limit allows for resonant passes to decay and permits a clear definition of the asymptotic behavior of the soliton. Care has to be taken not to exceed a certain time limit in order to prevent reflection from the boundaries. The asymptotic velocities, for the reflected and transmitted cases were calculated using the

actual motion of the center of the soliton and with the theoretical expressions for the kinetic and potential energies of the free soliton.

We chose the parameter $\lambda = m^2$ in eq. (1) without loss of generality and allowed three different values for $m = 0.7, 1, 1.5$ so chosen in order to study solitons whose effective widths $\approx \frac{1}{m}$ are bigger, comparable, and smaller than the barrier widths $\approx \frac{a}{6}$, where a is the parameter in the argument of $U(x)$ in eq. (3). For that purpose we took a repulsive barrier whose width is fixed at $a_1 = 1$ and an attractive barrier with $a_2 = 0.3$. The reason for this distinction was biased by our knowledge of the nuclear potential, that for heavy nuclei α decay has a deep and short range attractive well and much broader repulsive barrier generated by the Coulomb interaction. The choice of potential heights was determined by the desire to see all the effects in a range of reasonable velocities (not too low nor to high) around $v \approx 0.25$. Trial and error and the above considerations lead us to choose $h_1 = 1$ and $h_2 = -6$. The lack of analytical solutions for finite size barriers prevented us from general predictions and we therefore limited ourselves to the above parameter set.

Figure 1 shows the impinging soliton as well as the various barriers. Figures 2-5 show the final velocity v' as a function of initial velocity v for the repulsive $h_1 = 1, h_2 = 0$, attractive $h_1 = 0, h_2 = -6$, attractive-repulsive and repulsive-attractive cases respectively. The repulsive case of Fig.2 shows a clear particulate behavior. The soliton is reflected, $v' < 0$, up to a certain speed for which the effective barrier height becomes comparable with the kinetic energy and then there is a sudden jump to transmission. In all three cases the transmission starts at the same kinetic energy, with minor differences due to the effective barrier that is composed of the kink and the barrier. The attractive case of Fig. 3 is analogous to the δ function pattern found by Kivshar et al. [4]. There are islands of reflection in between trappings and resonant behavior for which the soliton remains inside the impurity and os-

cillates exciting the so-called impurity mode. Again the higher the mass, the smaller the critical velocity for which transmission starts. The details of the reflection islands depend strongly on the parameters but the general trend is analogous for all three mass cases. Figure 4 depicts the results for a combination of attractive and repulsive impurities. For low velocities reflection dominates -induced by the repulsive impurity-, then trapping and resonant behavior occurs with islands of reflection followed by transmission essentially dictated by the same impurity (Compare to Fig. 2). The repulsive-attractive case of Fig. 5 is similar to the repulsive case for velocities below transmission and the critical speed is here determined mainly by the attractive impurity that can drag back the soliton after it passes through the barrier. It appears that the larger the mass (the thinner the soliton) the attractive impurity is more capable of trapping, thereby producing a somewhat counterintuitive behavior for which the larger mass solitons tend to need a higher initial velocity in order to traverse them.

Concerning the permanence time inside the barrier, there is always a time delay in the impurities, in contradistinction to the quantum-mechanical Hartmann effect [7]. Also, energy is conserved in the scattering.

The present investigation addressed the one dimensional case. In order to relate more closely to actual nuclear (or optical) tunneling phenomena one has to consider higher dimensions, such as the $O(3)$ two- dimensional case or the skyrmion, including eventually rotations of the soliton and other effects, like fluctuations. Moreover, actual nuclear barriers are dynamical and not stiff. There is then a need to allow for more flexibility in the impurities as well as the possibility of dissipation.

Acknowledgements

It is a pleasure to thank Prof. Ignatovich from Dubna for a motivating question that triggered this project.

References

- [1] T.H.R. Skyrme, Proc. Roy. Soc. London, **A260** , 127 (1961); **A262**, 237 (1961) and Nucl. Phys. **31**,556 (1962).
- [2] G.S. Adkins, C.R. Nappi, and E. Witten, Nucl. Phys. **B228**, 552 (1983).
- [3] V. S. Olkhovsky and E. Recami, Phys. Reports **214**, 339 (1992).
- [4] Y. S. Kivshar, Z. Fei and L. Vazquez, Phys. Rev. Lett. **67**, 1177 (1991),
Z. Fei, Y. S. Kivshar and L. Vazquez, Phys. Rev. **A46**, 5214 (1992).
- [5] J. A. Gonzalez and B. de A. Mello, Phys. Scripta **54**, 14 (1996).
- [6] K. Fukushima and T. Yamada, Phys. Lett **A200**, 350 (1995).
- [7] T. E. Hartman, Phys. Rev. **33**, 3427 (1962).

Figure Captions

Fig. 1: From top to bottom: Kink with $m = 1$ impinging from the left onto a repulsive barrier. kink with $m = 1$ impinging from the left onto an attractive impurity. Kink with $m = 0.7$ impinging from the left onto an attractive-repulsive system. Kink with $m = 1.5$ impinging from the left onto a repulsive-attractive arrangement.

Fig. 2: Final velocity v' as a function of the initial velocity v for soliton mass parameters $m = 0.7$ upper curve $m = 1$ middle curve and $m = 1.5$ lower curve for the repulsive barrier.

Fig. 3: Same as figure 2 for the attractive case.

Fig. 4: Same as figure 2 for the attractive-repulsive case.

Fig. 5: Same as figure 2 for the repulsive-attractive case.

Fig. 1

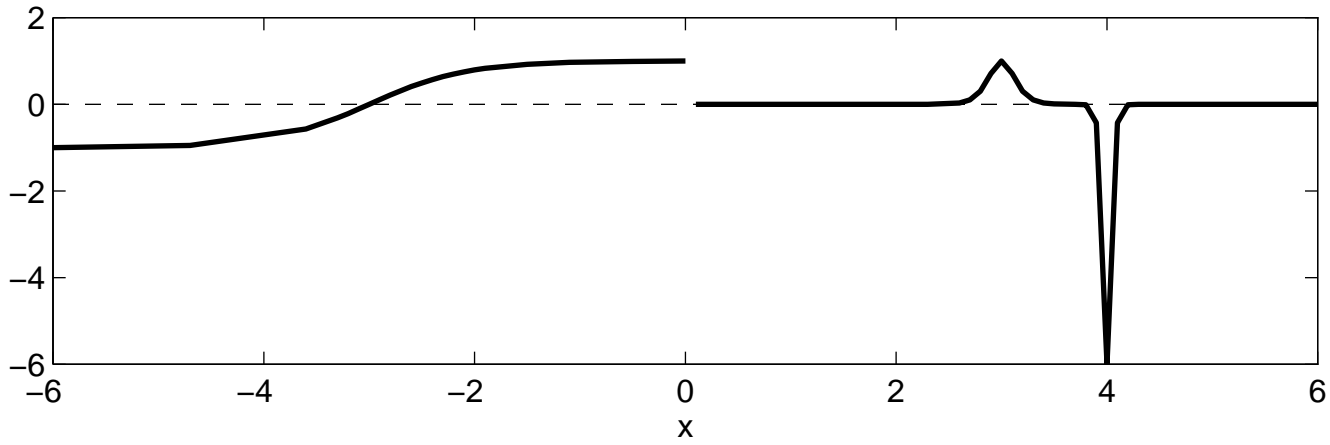
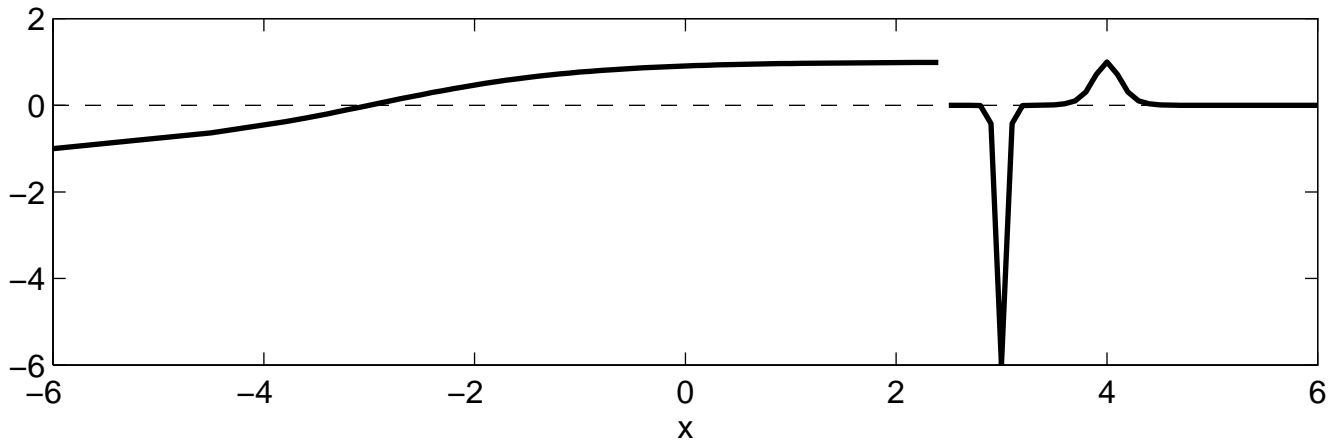
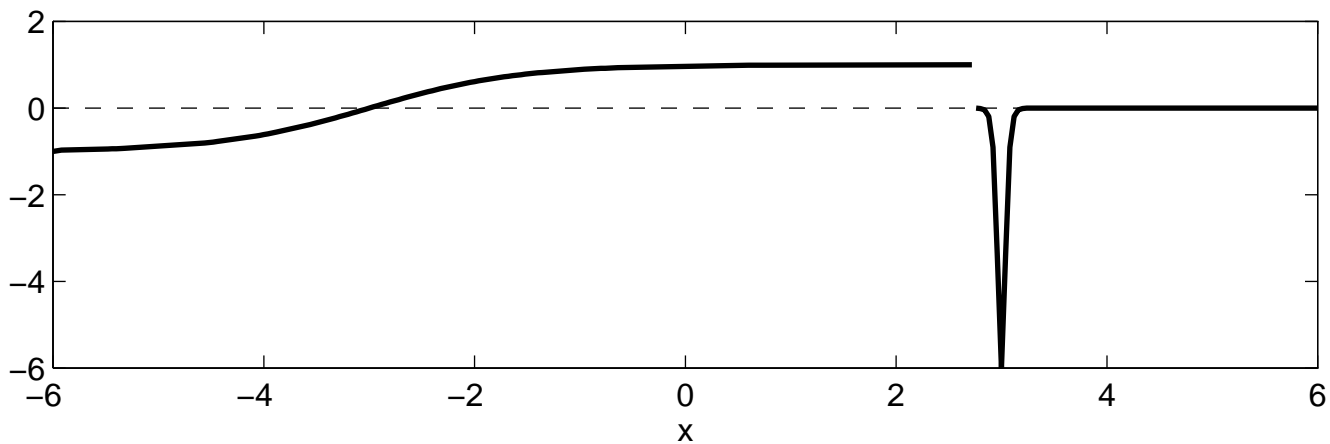
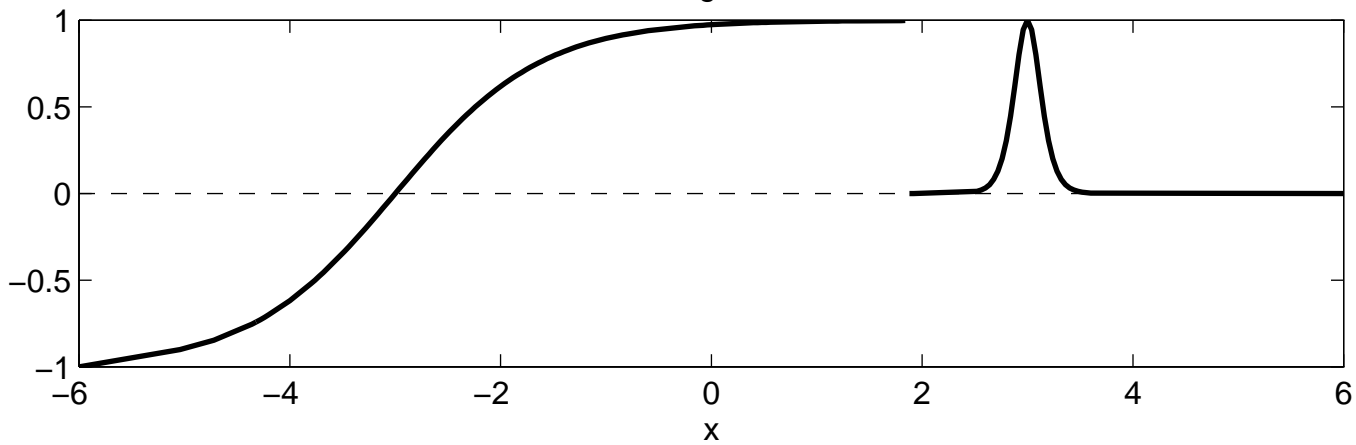


Fig. 2

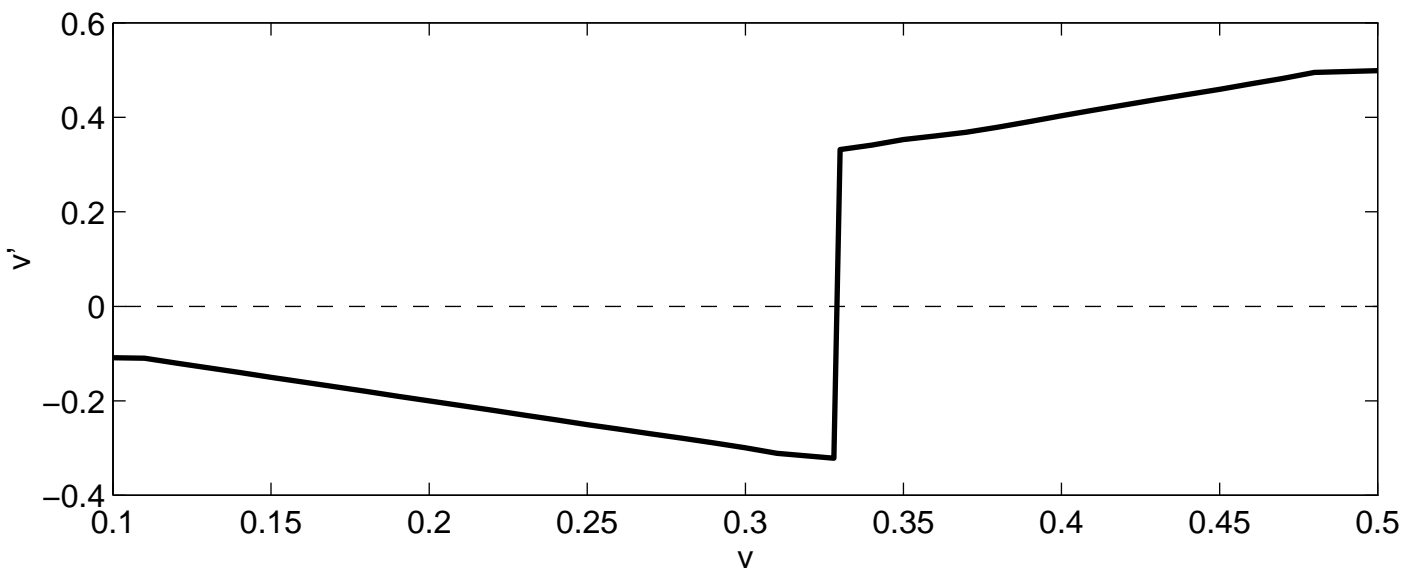
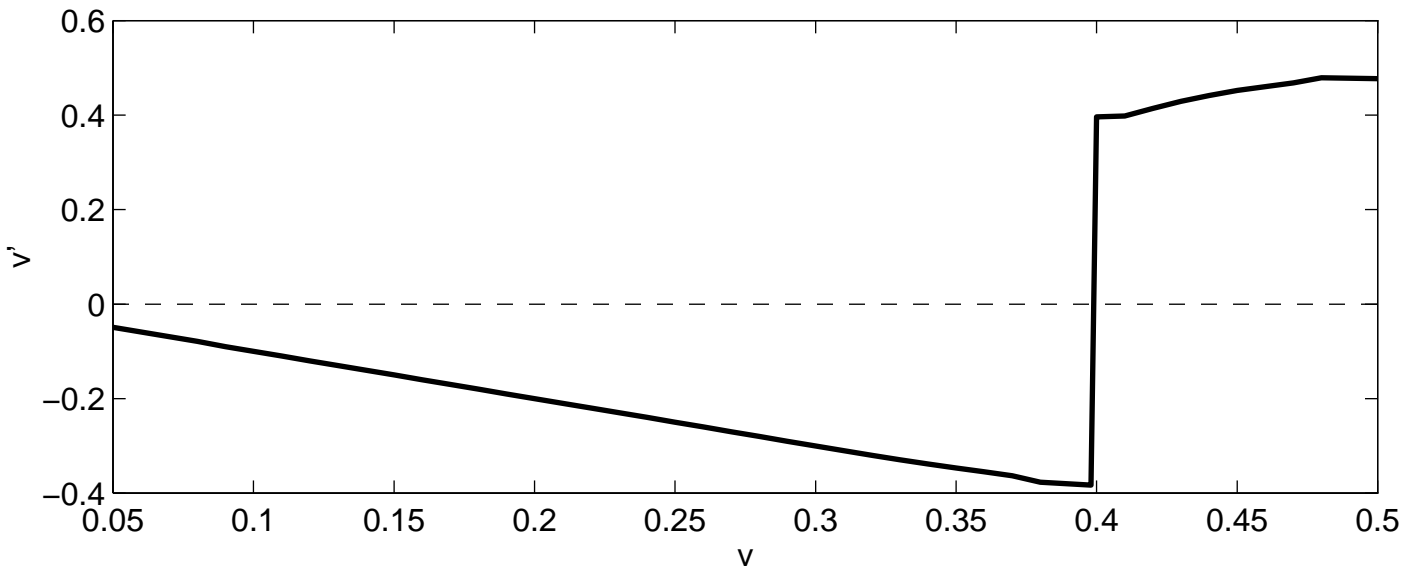
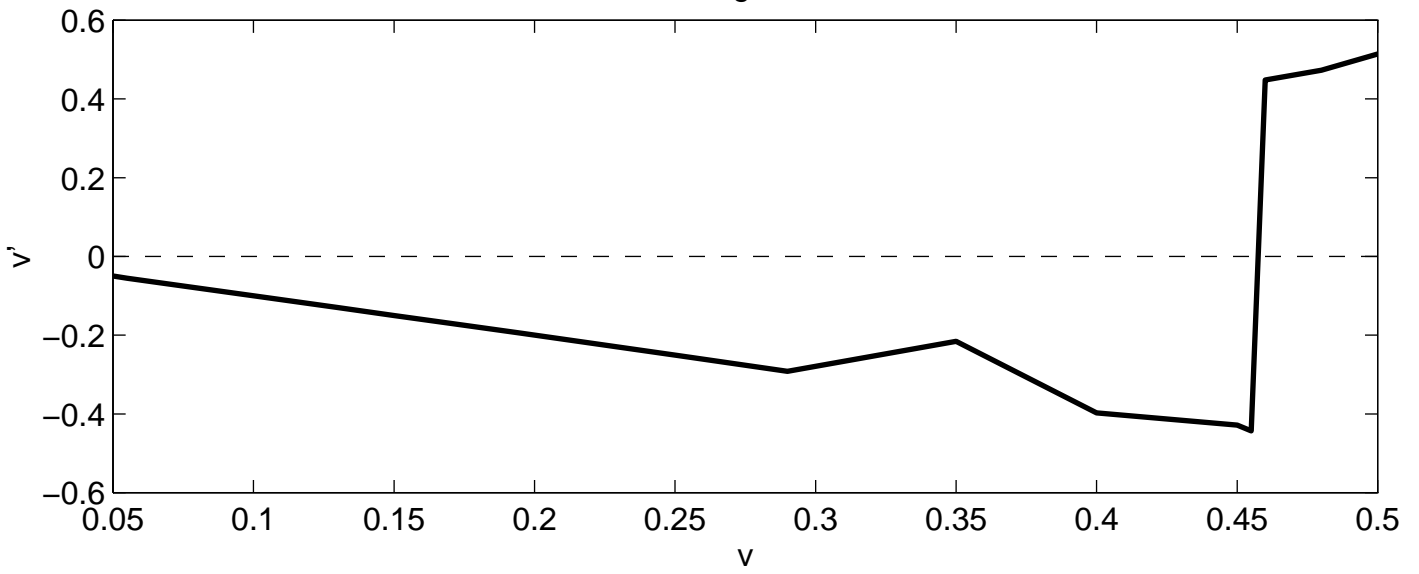


Fig. 3

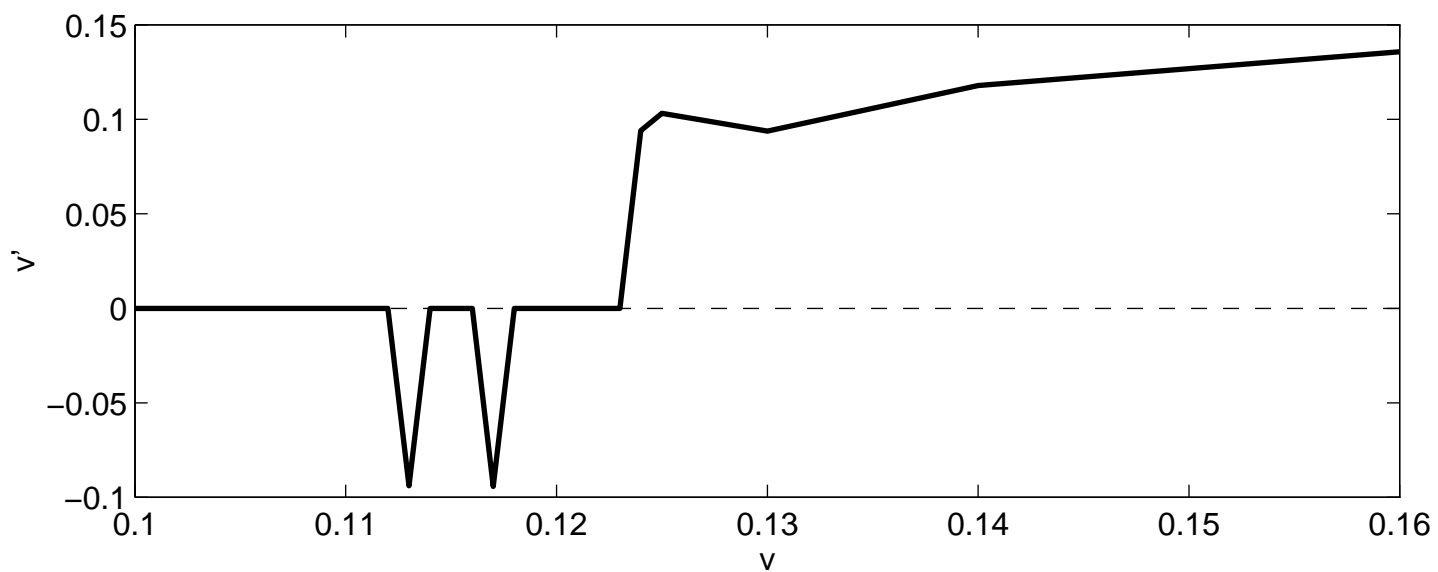
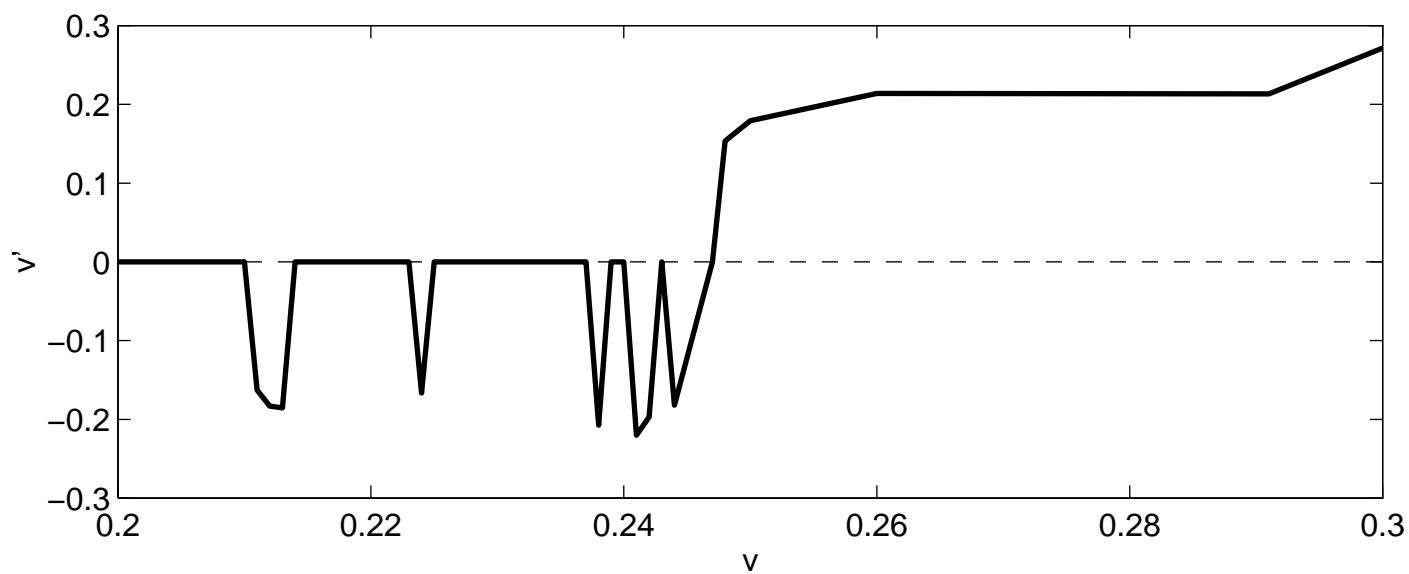
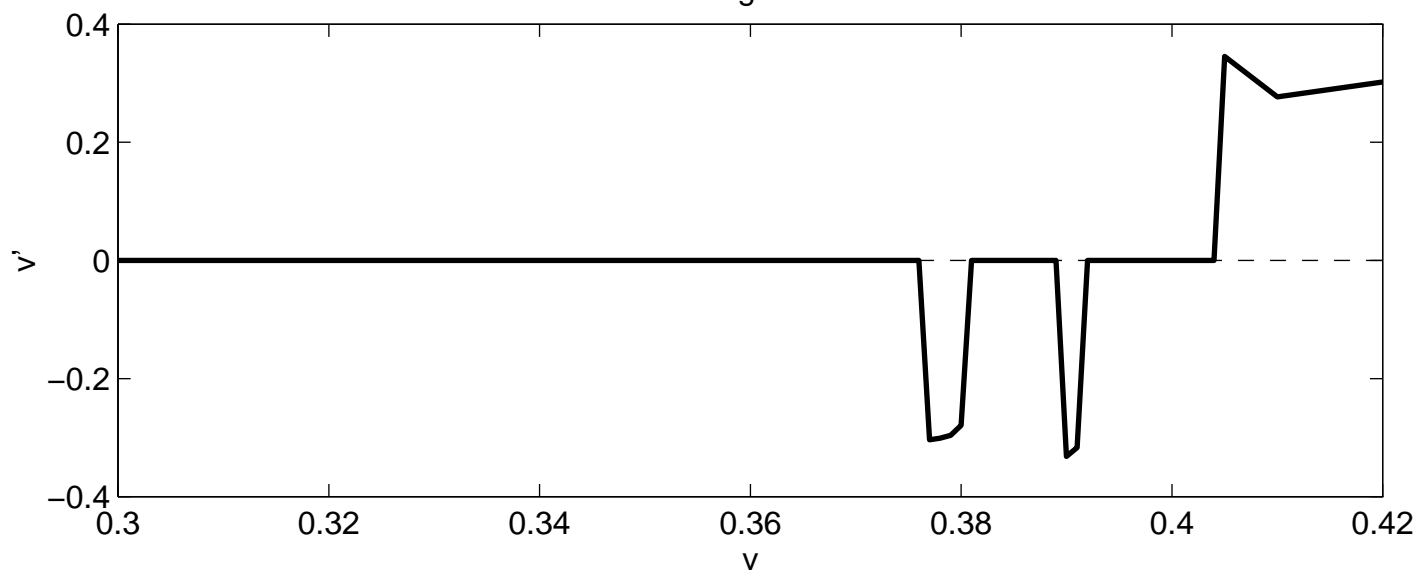


Fig. 4

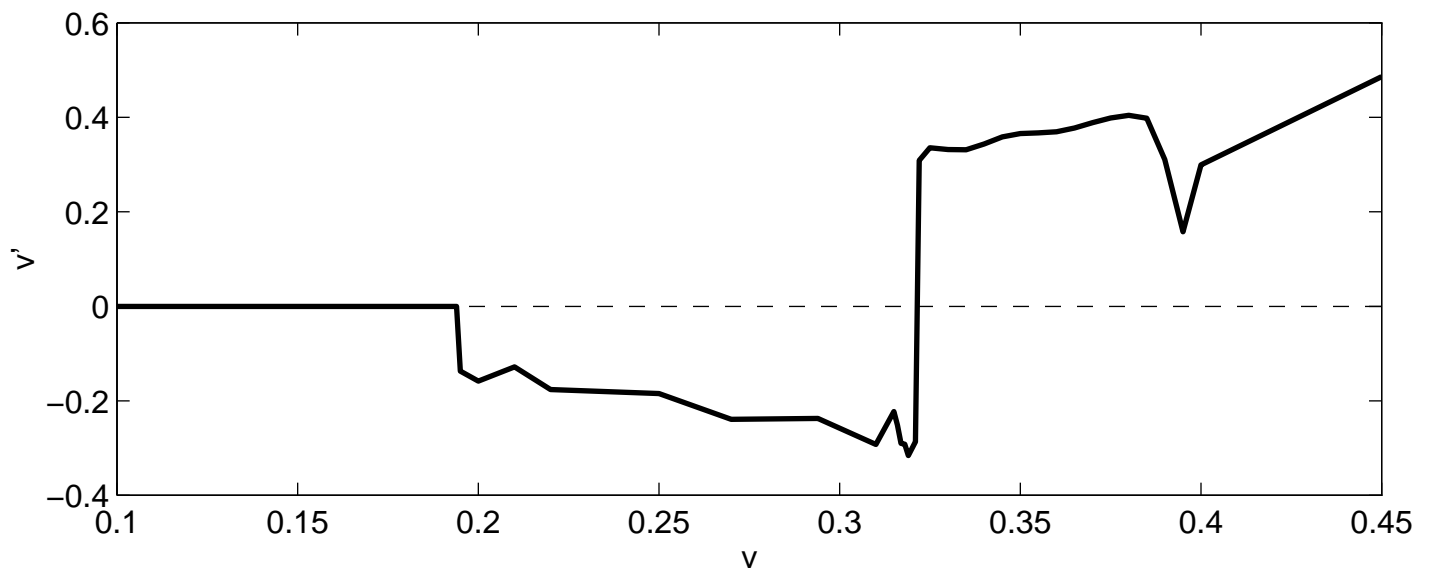
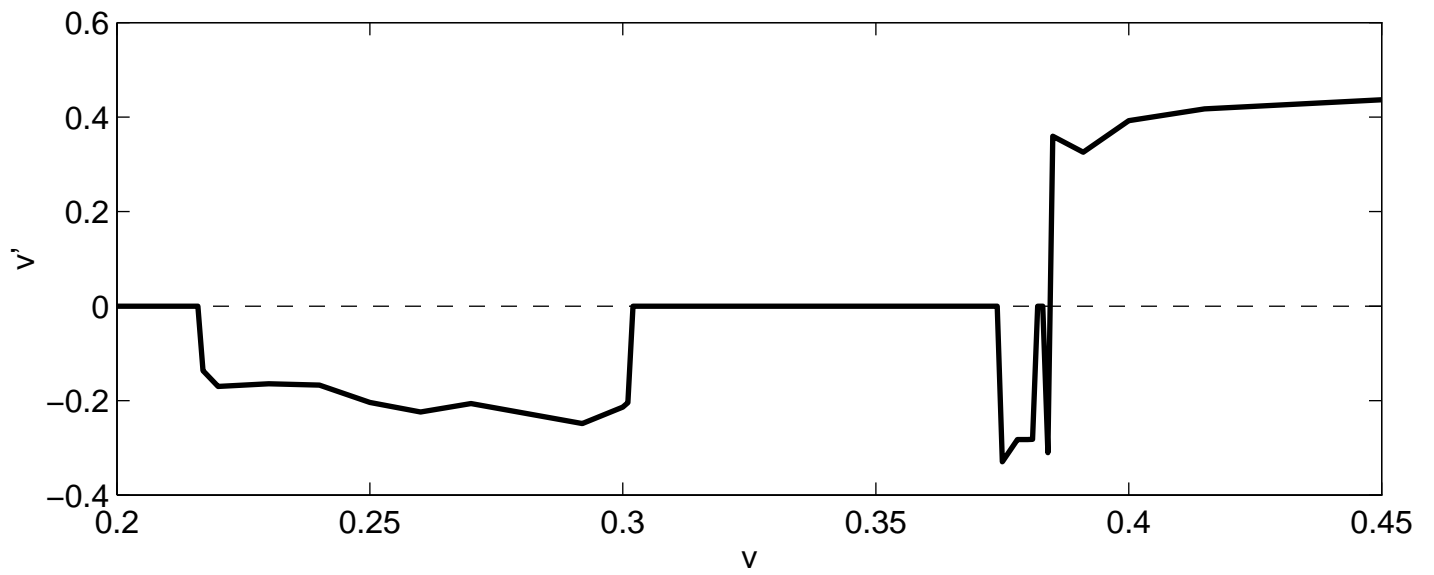
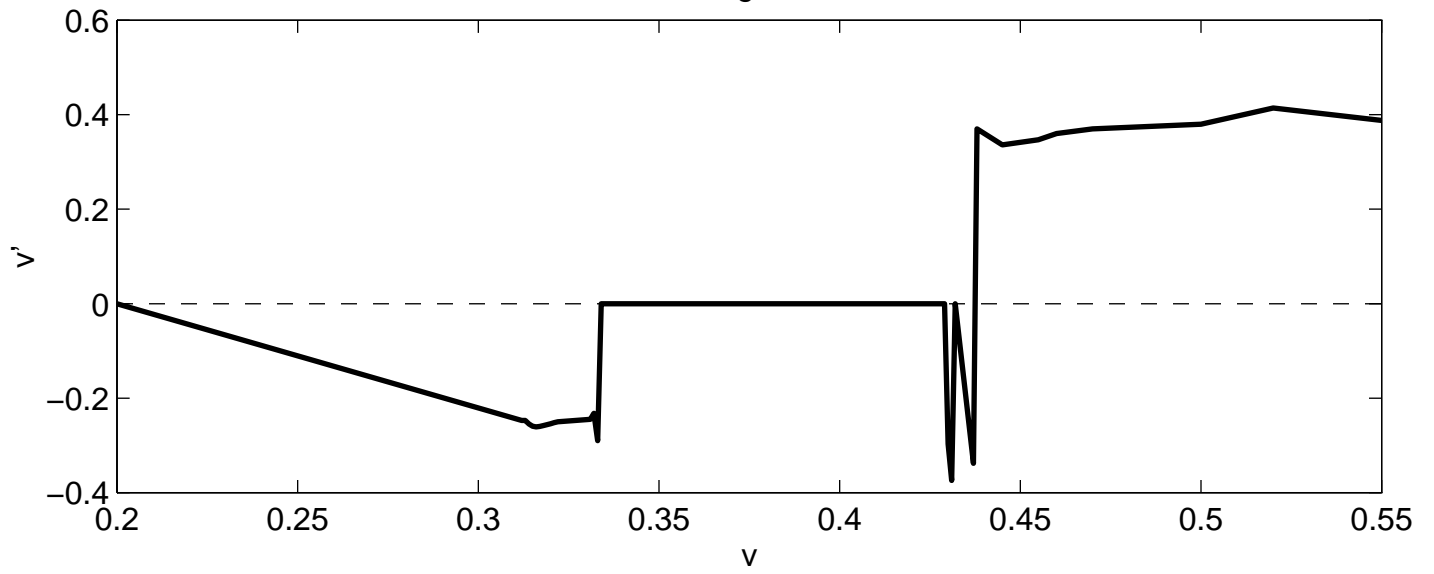


Fig. 5

